Accuracy analysis of tool deflection error modelling in prediction of milled surfaces by a virtual machining system

Mohsen Soori*, Behrooz Arezoo and Mohsen Habibi

CAD/CAPP/CAM Research Center,
Department of Mechanical Engineering,
Amirkabir University of Technology (Tehran Polytechnic),
424 Hafez Avenue, Tehran 15875-4413, Iran
Email: mohsen.soori@gmail.com
Email: m.soori@aut.ac.ir
Email: barezoo@yahoo.com
Email: arezoo@aut.ac.ir
Email: mohsen.habibi.mech@gmail.com
*Corresponding author

Abstract: Accuracy of produced parts in machining process is influenced by many errors such as tool deflection as well as geometrical deviations of machine tool structure. To increase accuracy and productivity in part manufacturing, the errors are modelled by using mathematical concepts. This paper presents an application for the virtual machining systems to analyse accuracy in modelling of tool deflection error. A virtual machining system is used to create actual parts in virtual environments. Then, a comparison for different methods of tool deflection error such as cantilever beam model of the cutting tool, Finite Element Method (FEM) of the cutting tool and workpiece and geometrical model of the cutting tool effects on the workpiece is presented to show accuracy and reliability of the methods in prediction of milled surfaces. So, capabilities and difficulties of the methods in the error modelling are presented to increase accuracy and efficiency in part manufacturing.

Keywords: virtual machining; tool deflection error; accuracy of error modelling; FEM; finite element method; three-axis CNC.

Reference to this paper should be made as follows: Soori, M., Arezoo, B. and Habibi, M. (2017) 'Accuracy analysis of tool deflection error modelling in prediction of milled surfaces by a virtual machining system', *Int. J. Computer Applications in Technology*, Vol. 55, No. 4, pp.308–321.

Biographical notes: Mohsen Soori received his MSc in Mechanical Engineering from Amirkabir University of Technology (Tehran Polytechnic), Tehran, Iran. His research interests are CAD/CAM, CIM and virtual manufacturing.

Behrooz Arezoo received his PhD in Mechanical Engineering from University of Sheffield, Sheffield, UK. He is currently Professor of Mechanical and Production Engineering in Amirkabir University of Technology (Tehran Polytechnic), Tehran, Iran. His research interests are CAD/CAPP/CAM and expert systems.

Mohsen Habibi received his PhD in Mechanical Engineering from Concordia University, Montreal, Canada. His research interests are CAD/CAM/CAE, additive manufacturing, gear manufacturing and CNC machine tools.

1 Introduction

The goal of present day manufacturing is to increase accuracy in produced parts with regard to the time and cost of part production. Accuracy of produced parts can be increased by a fewer manufacturing process errors in order to boost level of efficiency in part manufacturing. Since the product complexities have increased and product life cycle times have been reduced in competitive condition of marketing, the methods which can analyse parts in virtual environments

become more and more favourable. The concept of virtual machining is the ability of performing machining operations in a comprehensive simulation environment to obtain realistic predictions of error effects on the workpiece. It is created by simulating the actual machining in virtual environments using the real models of machine tools and workpiece as well as considering errors of machining operations presented by mathematical concepts. As a result, true sense of real machining experience can be presented in analyser software to control effects of manufacturing process errors on accuracy of produced parts.

Accuracy of produced parts as well as efficiency of part manufacturing using CNC machine tools are influenced by many errors. These include force and stress, geometrical deviations of machine tool structure, thermal variations, tool wear and servo errors. Geometrical and tool deflection errors which are inherited in machine tool structures have a big portion of the total volumetric error and are closely related to precision of produced parts. Identification and measurement of these errors are demand of precision machining in order to increase efficiency of part manufacturing. Therefore, a software which can simulate these errors in the virtual environment can provide a key tool in research for controlling and reducing the error effects. Also, accuracy in different methods of error modelling can be compared by using the virtual machining systems in order to present abilities as well as difficulties of the methods in prediction of milled surfaces.

2 Review of the research works

Fortunato and Ascari (2013) presented the virtual design of machining centres in order to provide a quick and easy analyse solution for machine tools design. A virtual machining system is presented by Altintas et al. (2005) in order to analyse and optimise elements of machine tools by using finite element models. A new methodology in machining of low-rigidity components is presented by Ratchev et al. (2003) to predict and compensate surface errors due to deflection error. To predict and analyse errors of milled surfaces in milling operations, a developed virtual machining system is presented by Yun et al. (2002).

The influences of different cutting conditions, cutting styles and cutting modes to the cutting forces are investigated by Ikua et al. (2001) to predict cutting forces as well as machining errors in ball-end milling of curved surfaces. In order to increase material removal rate in milling operations, a generalised process simulation as well as optimisation strategy for two 1/2-axis milling machines is presented by Altintas and Merdol (2007).

A methodology is presented by Habibi et al. (2011) to enhance accuracy of produced parts by compensation of the tool deflection and geometrical errors. An enhancement in tool paths accuracy of CNC milling machine using geometrical error compensation is presented by Nojedeh et al. (2011) to eliminate tool path deviations created by geometrical as well as kinematical errors. Eskandari et al. (2013) introduced an innovative error compensation method by modification of NC codes to compensate the volumetric errors due to positional, geometrical and thermal errors of CNC milling machine.

A virtual machining system by considering dimensional and geometrical errors of a three-axis CNC milling machine is presented by Soori et al. (2013) to create actual machined parts in virtual environments. Soori et al. (2014) presented virtual machining by considering dimensional, geometrical and tool deflection errors in three-axis CNC milling machines in order to create actual machined parts in the virtual environments. Application of virtual machining systems in monitoring and minimising the tool deflection error of three-axis CNC milling machines is presented by Soori et al. (2016).

A generalised process simulation and optimisation strategy using a virtual cutting system is presented by Merdol and Altintas (2008) to predict and improve the performance of three-axis milling operations. Cao and Altintas (2007) presented an integrated model of spindle bearing as well as machine tool system by consisting shaft rotation, tool holder, angular contact ball bearings, housing and the machine tool mounting.

Application of tool deflection knowledge in process planning is presented by Ong and Hinds (2003) to meet desired geometric tolerances by selecting optimal feed rates. Tool deflection error compensation in peripheral milling of curved geometries is presented by Rao and Rao (2006) in order to increase accuracy in machining of curved geometries.

In order to compensate the machining errors due to tool deflection error, a strategy is proposed by Dépincé and Hascoët (2006a) which can modify nominal positions of cutting tool along machining paths. A new methodology in selection of milling tool paths in machining of complex surfaces is presented by de Lacalle et al. (2007) to minimise dimensional errors due to the tool deflection error.

To improve the design quality of the feed drive system in CNC machine tools, an integrated design and analysis system is presented by Liu and Wang (2016). Construction of a virtual reality environment for robotic manufacturing cells is presented by Gogouvitis and Vosniakos (2015). Interpretation-oriented information interface for manufacturing enterprises is presented by Chen and Zhao (2016) to improve level of understanding about product life cycle as well as enterprise management.

Effect of tool setting error on the topography of surfaces machined using peripheral milling is presented by Arizmendi et al. (2009). In order to increase accuracy of produced parts in boring operations, force and deformation model for error correction is presented by Arsuaga et al. (2012).

All of the research works on the tool deflection error presented so far have focused on the modelling as well as compensating the errors (Ratchev et al., 2003; Yun et al., 2002; Ikua et al., 2001; Habibi et al., 2011; Dépincé and Hascoët,

2006a). In order to decrease the tool deflection error in machining processes, optimisation techniques are also used in research works (Soori et al., 2016; Ong and Hinds, 2003; Merdol and Altintas, 2008). According to the author's findings, it was concluded that accuracy of the presented methods in tool deflection error modelling in comparison to the other methodologies were insufficiently explored in the previous works. Also, the capabilities and difficulties of the presented methods in the tool deflection error modelling were not studied.

In the present research work, an application for the virtual machining systems is presented in order to evaluate accuracy as well as reliability of tool deflection error modelling. The aim is to enhance quality of produced parts as well as efficiency of part manufacturing by using the most appropriate method of tool deflection error modelling in prediction of milled surfaces. So, a comparison for different methods of tool deflection error such as cantilever beam model of the cutting tool, Finite Element Method (FEM) of the cutting tool and workpiece and geometrical model of the cutting tool effects on the workpiece is presented by using a virtual machining system to show their accuracy in error modelling. As a result, capabilities and difficulties of the considered methods in the tool deflection error modelling are presented in order to increase accuracy as well as efficiency of part manufacturing by using the most appropriate method.

A virtual machining system which can enforce tool deflection error of three-axis CNC milling machines is used to create actual parts in the virtual environments. The tool deflection error is enforced on G-Codes of parts to produce real 3D model of the parts in virtual environment. Different methods of the tool deflection error modelling are used in order to present the accuracy and reliability of the methods in prediction of the milled surfaces. The obtained results are compared by charts and diagrams in order to present abilities and difficulties of the methods. As a result, capabilities and difficulties of the considered methods in the tool deflection error modelling are presented by a virtual machining system in order to improve accuracy and efficiency of part manufacturing.

In Section 3, modelling of cutting forces for flat end milling tools is presented. Different methods of the tool deflection error modelling in prediction of the milled surfaces are described in Section 4. The algorithm of the virtual machining software to enforce the tool deflection error is presented in Section 5. Finally in Section 6, the validation of the developed algorithms in accuracy analysis of tool deflection error modelling is described by comparing the errors of machined parts with a free from profile in real and virtual environments.

3 Modelling of cutting forces

Engin and Altintas (2001) presented a cutting force model by mathematical equations which can be parametrically defined for different helical end mills. So, cutting force equations for any type of cutting tools can be obtained by substituting values in the equations for those parameters according to tool envelop geometry. A typical milling operation with a general end mill is shown in Figure 1, where φ_{pj} is pitch angle of flute j, $\varphi_j(z)$ is total angular rotation of flute j at level z on the XY plane, $\psi(z)$ is radial lag angle and $\kappa(z)$ is axial immersion angle. In the differential chip, dz is differential height of the chip segment, ds is the length of cutting edge and h_j is height of valid cutting edge from tool tip.

Figure 1 Mechanics and kinematics of three-axis milling (see online version for colours)

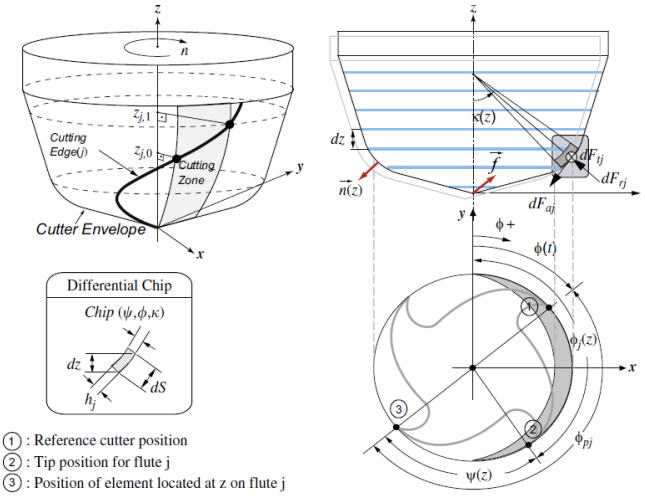

The differential tangential (dF_t), radial (dF_r) and axial (dF_a) cutting forces acting on an infinitesimal cutting edge segment are given in equation (1).

$$\begin{cases} dF_t = K_{te}ds + K_{tc}h\left(\phi_j,k\right)db \\ dF_r = K_{re}ds + K_{rc}h\left(\phi_j,k\right)db \\ dF_a = K_{ae}ds + K_{ac}h\left(\phi_j,k\right)db \end{cases} \quad (1)$$

where $h\left(\phi_j,k\right)$ is the uncut chip thickness normal to the cutting edge and varies with the position of the cutting point and cutter rotation.

The edge cutting coefficients K_{te}, K_{re} and K_{ae} are constants and related to the cutting edge length ds. The shear force coefficients K_{tc}, K_{re} and K_{ac} are identified either mechanistically from milling tests conducted (Fu et al., 1984; Yucesan and Altıntaş, 1996) or by a set of orthogonal cutting tests using an oblique transformation method presented by Budak and Tekeli (2005). Sub-indices (c) and (e) represent shear and edge force components, respectively.

The cutting force coefficients, especially the edge (K_{te}, K_{re}, K_{ae}) and radial (K_{rc}), increase with tool wear, hence they can be calibrated with a worn tool in order to consider the influence of wear on the process.

Coefficients of the edge cutting as well as the shear force are obtained in Section 6 by an experimental operation to validate the present research work. db is the projected length of an infinitesimal cutting flute in the direction along the cutting velocity which can be shown as equation (2).

$$db = \frac{dz}{SinK} \quad (2)$$

Details of *db* and uncut chip thickness $h(\phi_j, k)$ are shown in Figure 2.

Figure 2 Uncut chip thickness (see online version for colours)

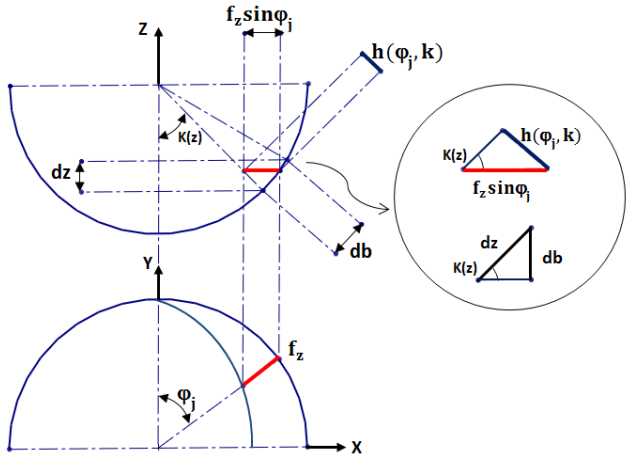

The geometric model is used to evaluate the positions of the cutting points along the flute. In order to identify the location of the same flute point on the cut surface, the rigid body kinematics as well as structural displacements of the cutter and workpiece are used. Chip load should be identified and cutting coefficients should also be evaluated for the local edge geometry. Then, the cutting forces in Cartesian coordinate system can be evaluated as equation (3).

$$\begin{bmatrix} dF_x \\ dF_y \\ dF_Z \end{bmatrix} = \begin{bmatrix} -\sin\phi_j \sin\kappa & -\cos\phi_j & -\sin\phi_j \cos\kappa \\ -\cos\phi_j \sin\kappa & \sin\phi_j & -\cos\phi_j \cos\kappa \\ \cos\kappa & 0 & -\sin\kappa \end{bmatrix} \begin{bmatrix} dF_r \\ dF_t \\ dF_a \end{bmatrix} \quad (3)$$

The total cutting forces for the rotational position φ_j can be found by integrating as equation (4).

$$\begin{cases} F_x(\phi_j) = \sum_{j=1}^{N_f} F_{xj}\left[\phi_j(z)\right] \\ \quad = \sum_{j=1}^{N_f} \int_{Z_1}^{Z_2} \left[-dF_{rj} \sin\phi_j \sin\kappa_j - dF_{tj} \cos\varphi_j \right. \\ \quad \left. -dF_{aj} \sin\phi_j \cos\kappa_j \right] dz \\ F_y(\phi_j) = \sum_{j=1}^{N_f} F_{yj}\left[\phi_j(z)\right] \\ \quad = \sum_{j=1}^{N_f} \int_{Z_1}^{Z_2} \left[-dF_{rj} \cos\phi_j \sin\kappa_j + dF_{tj} \sin\phi_j \right. \\ \quad \left. -dF_{aj} \cos\phi_j \cos\kappa_j \right] dz \\ F_z(\phi_j) = \sum_{j=1}^{N_f} F_{zj}\left[\phi_j(z)\right] = \sum_{j=1}^{N_f} \int_{Z_1}^{Z_2} \left[dF_{rj} \cos\kappa_j - dF_{aj} \sin\kappa_j \right] dz \end{cases} \quad (4)$$

where N_f is the number of flutes on the cutter, z_1 and z_2 are the contact boundaries of the flute which is in the cutting tool and κ_j is axial immersion angle of flute *j*.

In the flat end mill the $\kappa = 90°$, thus the cutting force of equation (4) can be simplified as equation (A1) in Appendix A.

4 Tool deflection models

The tool deflection error is created by moving away of milling tool from theoretical position of G-codes due to enforce cutting forces in milling operations. Accuracy of milled surfaces and desired surface roughness in milling operations are influenced by the tool deflection error. Also, the excessive amount of tool deflection can cause failures of the cutting tool or even seriously defects of the workpiece.

In order to compute the tool deflection, three are several models as below:

- Cantilever beam model of the cutting tool: A cutting force model which is concentrated to the points of enforced forces to the cutting tool while the points have to be chosen or distributed along the cutting edge of the cutting tool.
- Finite Element Method (FEM) of the cutting tool and workpiece.
- A geometrical model of the cutting tool effects on the workpiece: Approach based on evolution of the contact points between the cutting tool and workpiece.

In the present study, the results of these different models are obtained by using a virtual machining system in order to compare accuracy as well as reliability of the methods in modelling the error.

4.1 Cantilever beam model of the cutting tool

Ryu et al. (2003) presented another method for calculation of the tool deflection error according to the tool rotational angle and the axial position. In order to calculate the tool deflection error more accurately, the machine tool deformation due to the deformation of tool clamping parts such as collet and arbour are considered. Deformations affecting the surface form error are combined factors of bending deformation (*dt*) of tool itself, and machine tool part deformation (*dc*). The deformation of machine tool part *dc* can be introduced by the longitudinal stiffness k_1 and rotational stiffness k_2. The force centre is established at the position in which the moments generated by all the infinitesimal cutting forces and by the equivalent point forces are the same at the intersectional face between the tool and collet (Ryu et al., 2003). Consequently, the value of tool deflection error is acquired from the equation (5) including the machine tool part deformation.

$$\begin{aligned} \delta = \delta_t + \delta_c &= \frac{F}{6EI}\left[-\left(L-L_f\right)^3 + 3\left(L-L_f\right)^2\left(L-z_f\right)\right] \\ &+ \frac{F}{6EI_f}\left[\left(z_f-z\right)^3 - \left(L_f-z\right)^3 + 3\left(L_f-z\right)^2\left(L_f-z_f\right)\right] \\ &+ \frac{F}{2EI}\left[-\left(L-L_f\right)^2 + 2\left(L-L_f\right)\left(L-z_f\right)\right]\left(L_f-z\right) \\ &+ \frac{F\left(L-z_f\right)\left(L-z\right)}{K_2} + \frac{F}{K_1} \end{aligned} \quad (5)$$

where E is the modulus of elasticity (MPa) of the tool material, I is the equivalent moments and $K = \frac{AE}{L}$ for the relevant elements, while E, L and A refer to modulus of elasticity, length and area of element, respectively. Figure 3 shows elements of tool deflection method for equation (5).

Figure 3 Elements of tool deflection method of equation (5) (see online version for colours)

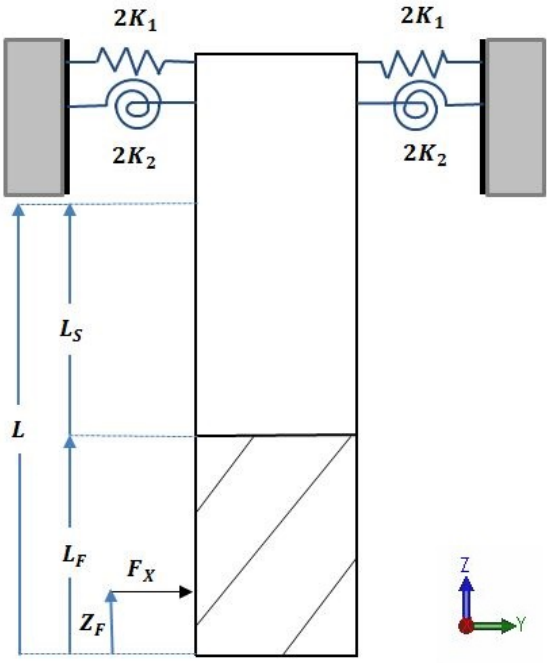

4.2 Finite element method (FEM)

To calculate deflection errors caused by cutting forces using the FEM, CAD models of the workpiece and cutting tool should be created. Then, the CAD models are divided to small elements by the mesh generation methods. The accuracy of error calculations by FEM is influenced by the workpiece and cutting tool mesh generated by the CAD software. Predicted cutting forces are applied to the each node of the meshed CAD models in order to calculate displacement of the node. Also, materials properties of the workpiece as well as cutting tool should be considered in the error calculation. As a result, the amount of node displacement due to applied forces to the meshed workpiece as well as cutting tool can be calculated.

4.2.1 Finite element modelling of the workpiece

Tsai and Liao (1999) presented a finite element model in order to analyse surface dimensional errors of thin-walled workpiece and cutting tool due to cutting forces. Also, Saffar et al. (2008) presented prediction of cutting forces and tool deflection error by the FEM.

Figure 4 shows the considered surfaces of the workpiece in the milling operation as transient surface and machined surface for analysing by the FEM.

Figure 4 The considered surfaces of the workpiece in the milling operation for the FEM analysis (see online version for colours)

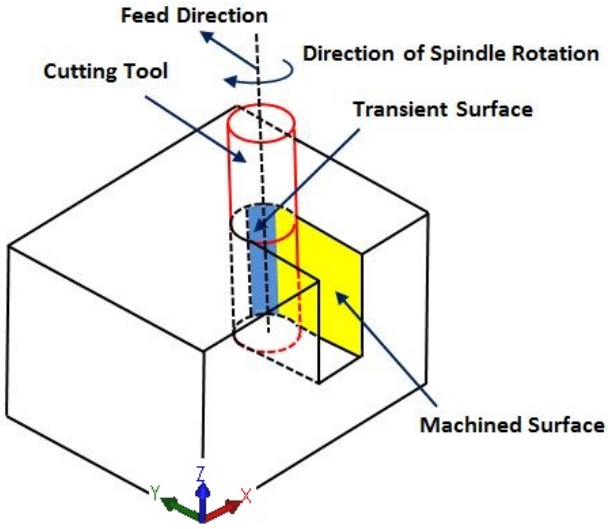

Then, finite-element discretisation of the workpiece surfaces is generated as is shown in Figure 5.

Figure 5 Finite-element discretisation of the workpiece surfaces (see online version for colours)

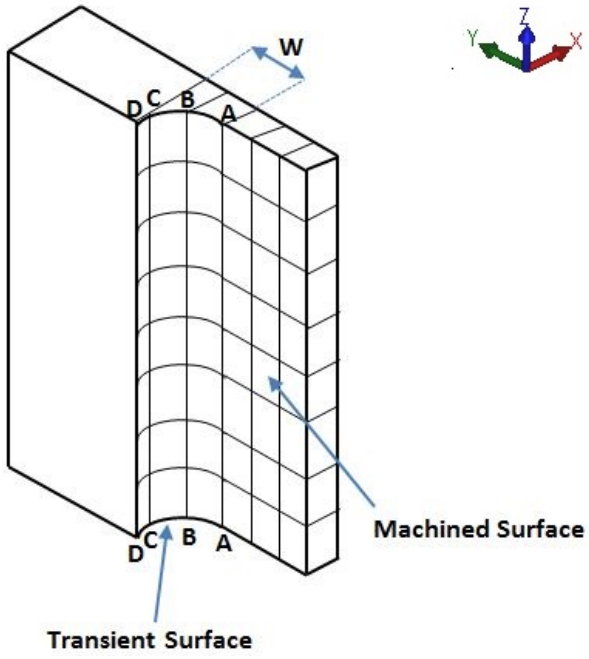

There are three nodes in the Y direction and two nodes for the X and Z direction for the each 3D element of workpiece which are presented in Figure 5. Three degrees of freedom as the three displacements of (u_x, u_y, u_z) are considered for each node in the 3D finite-element mesh. In order to obtain the error form of the machined surface, deflection of the cutting tool as well as the deformation of the workpiece along the A-A line as is shown in Figure 6 should be calculated.

When the cutting edges of the cutting tool touch the nodal point of the workpiece, the height of the error form on the machined surfaces can be described as equation (6) (Tsai and Liao, 1999).

$$x_l = \frac{\left(\frac{2\pi}{N_f}\right)}{\beta_0} \tag{6}$$

where N_f is the number of flutes on the end milling cutter.

The X_l is equal to zero when the first cutting edge of the cutting tool approaches to the line A-A at the bottom position of the cutting tool. As a result, the machined surface is generated from the bottom of the workpiece by cutting edges of the cutting tool.

The error form of machined surface of the workpiece in the down milling operation can be described as equation (7) (Tsai and Liao, 1999).

$$e(X_l, Z_l) = \delta Y_t(i,j,l) + \delta Y_w(X_i, j, Z_l) \tag{7}$$

where the height of the surface form error is as equation (8) (Tsai and Liao, 1999).

$$X_l = (i-1)D_x \tag{8}$$

where i is the number of axial segment. Also, the rotation angle of the cutting tool is as equation (9) (Tsai and Liao, 1999).

$$\theta_j = (j-1)\theta_{Dx} \tag{9}$$

where j is the number of angular step which is equal to i.

Thus, the error form of machined surfaces of the workpiece at the feed location Z_l can be obtained by repeating the simulation for every θ_{Dx} angular increment over one flute passing period $\frac{2\pi}{N_f}$ in equation (7) for all of the nodal points at line A-A of the workpiece.

To determine the cutting forces acting on the each axial segment of the workpiece as is shown in Figure 5, the chip thickness of the helical fluted end mill for the flute K-th, the axial segment of i-th and angular position of j-th can be considered as equation (10) (Tsai and Liao, 1999).

$$h(i,j,k) = f_t \sin\beta(i,j,k) \tag{10}$$

where f_t is the feed per cutting edge. Also, $\beta(i,j,k)$ is the rotation angle of the cutting tool for the flute k, the axial segment of i and angular position of j which can be presented as equation (11) (Tsai and Liao, 1999).

$$\beta(i,j,k) = \left[-\theta_{(j)} + \frac{2\pi(k-1)}{N_f}\right] + \delta\lambda \tag{11}$$

where θ_j is the rotation angle of the j-th angular position, N_f is the number of flutes on the end milling cutter. Also, $\delta\lambda$ can be expressed as equation (12) (Tsai and Liao, 1999).

$$\delta\lambda = x_1 \tan\frac{\alpha_h}{R} \tag{12}$$

where α_h is the helix angle of the helical cutting tool, R is radius of the cutting tool. Also, x_1 can be explained by equation (13) (Tsai and Liao, 1999).

$$x_1 = (i-1)D_x + \frac{D_x}{2} \tag{13}$$

So, tangential cutting force (dF_t) and radial cutting force (dF_r) can be presented as equation (14) (Tsai and Liao, 1999).

$$\begin{cases} dF_t = K_S D_x h(i,j,k) \\ dF_r = K_r K_S D_x h(i,j,k) \end{cases} \tag{14}$$

where K_s is constant for the specific cutting force and K_r is ratio of the radial force to the tangential force. As a result, the cutting forces in the X and Y direction for each axial segment of the workpiece as is shown in Figure 5 can be explained as equation (15) (Tsai and Liao, 1999).

$$\begin{cases} dF_x = dF_t \sin\beta(i,j,k) + dF_r \cos\beta(i,j,k) \\ dF_y = dF_t \cos\beta(i,j,k) - dF_r \sin\beta(i,j,k) \end{cases} \tag{15}$$

The helical cutting edge of the cutting tool is not fully engaged with the workpiece. Section a-p of the line a-b on the helical cutting edge is not engaged with the workpiece as is shown in Figure 6. Engagement of the helical cutting edge of the cutting tool to the workpiece is shown in Figure 6.

Figure 6 Engagement of the helical cutting edge of the cutting tool to the workpiece (see online version for colours)

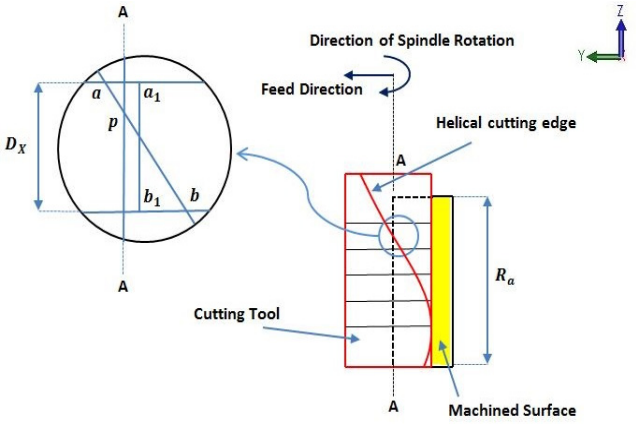

So, the cutting forces of the axial segments which are partially engaged with the workpiece and cutting edges should be modified by the correcting factor u as is presented in equation (16).

$$u = \frac{\beta_s - \left[\beta(i,j,k) - \theta_{Dx}/2\right]}{\theta_{Dx}} \tag{16}$$

where β_s is the start angle of cutting, β_e is the exit angle of cutting and θ_{Dx} is the projective angle of the helical flutes on the line a-b. Details of cutting starting angle and projective angle of the helical flute is shown in Figure 7.

Figure 7 Details of cutting starting angle and projective angle of the helical flute (see online version for colours)

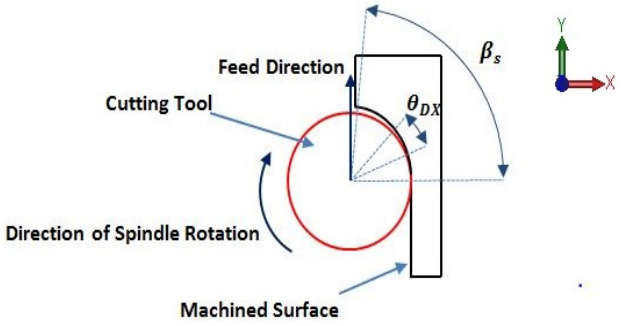

The cutting forces which are acting on the each axial segment engaged to the workpiece can be presented as equation (17) (Tsai and Liao, 1999).

$$\begin{cases} dF_x = \sum_{i=1}^{N_x}\sum_{k=1}^{N_f}\left[dF_t \sin\beta(i,j,k) + dF_r \cos\beta(i,j,k)\right]\delta(i,j,k) \\ dF_y = \sum_{i=1}^{N_x}\sum_{K=1}^{N_f}\left[dF_t \cos\beta(i,j,k) - dF_r \sin\beta(i,j,k)\right]\delta(i,j,k) \end{cases} \quad (17)$$

where $\delta(i,j,k)$ is presented in equation (18) (Tsai and Liao, 1999).

$$\delta(i,j,k) = \begin{cases} 1 & \beta_e < \beta(i,j,k) < \beta_S - \dfrac{\theta D_x}{2} \\ u & \beta_S - \dfrac{\theta D_x}{2} < \beta(i,j,k) < \beta_S + \dfrac{\theta D_x}{2} \\ 0 & \textit{Otherwise} \end{cases} \quad (18)$$

The flow chart to determine the error form of machined surfaces of the workpiece by using the FEM is presented in Figure 8.

4.2.2 *Finite element modelling of the cutting tool*

A new CAD/CAM/CAE integration approach is presented by Wang and Chen (2014) to predict tool deflection of end mills by using the FEM. Zeroudi and Fontaine (2015) presented prediction of tool deflection error and tool path compensation in ball-end milling by the FEM.

Figure 8 The flow chart to determine the error of machined surfaces of the workpiece by using the FEM

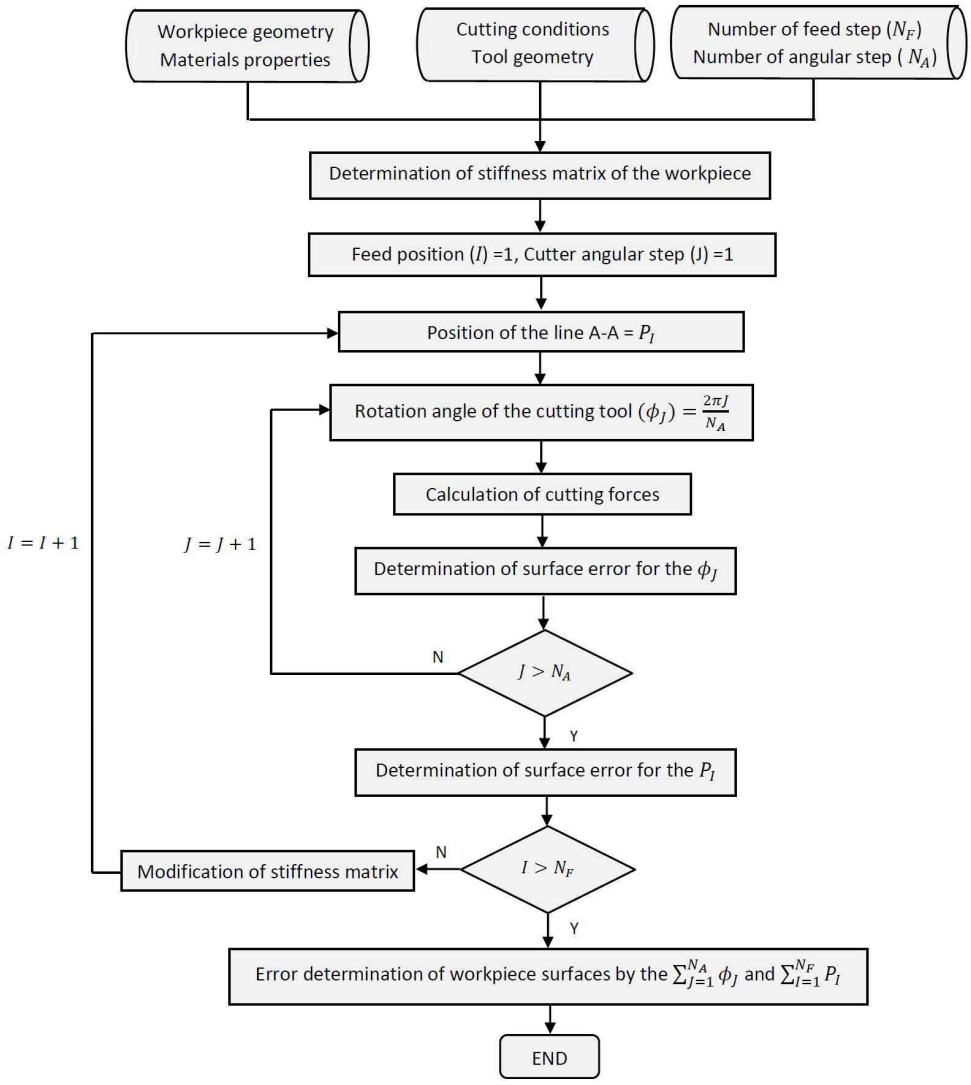

To calculate the tool deflection error by the FEM, CAD model of the cutting tool is divided into small elements by using the mesh generation methods. So, the tool deflection error can be calculated as equation (19) (Wang and Chen, 2014) via summing up the effects caused by the applied forces to the each node of the meshed CAD model.

$$dz = \sum_{i=1}^{M} d_i(z) \tag{19}$$

where d_i is deflection of each node of cutting tool created by applying cutting forces for each position of cutting tool along machining paths. As a result, amount of the tool deflection error due to applied cutting forces in milling operation can be calculated.

4.3 Approach based on evolution of the contact points between cutting tool and workpiece

Dépincé and Hascoët (2006a) presented a method in obtaining the simulated surface due to the tool deflection error based on evolution of the contact points between the cutting tool and workpiece. Also, a methodology in compensation of tool deflection error is presented by Dépincé and Hascoët (2006b) in order to achieve specific tolerances in milling operations. To determine the milled surface, the variation of the contact points between the workpiece as well as the cutting tool flute is considered. Then, the milled surface can be passed between the obtained contact points by applying a linear interpolation. The simulated error surface obtained by using the methods of contact points for three conditions of the deflected cutting tool is shown in Figure 9.

Figure 9 The simulated error surface obtained by using the method of contact points for three conditions of the deflected cutting tool (see online version for colours)

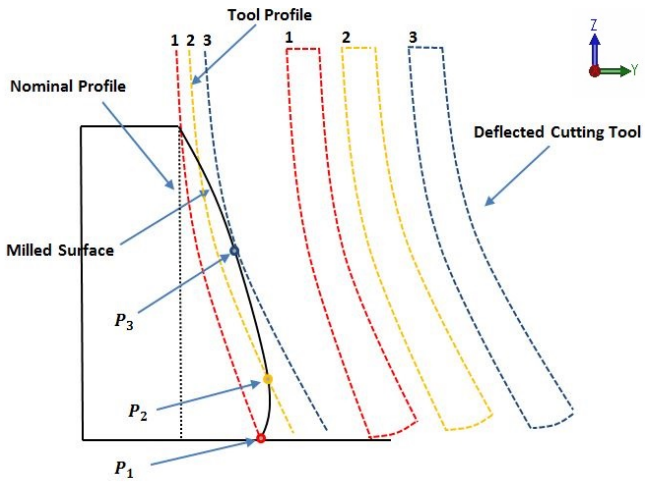

The two considered positions of the cutting tool during the machining of a plane at a constant feed are presented in Figure 10.

Points A and B are two contact points between profile of machining and the workpiece for the two considered positions of the cutting tool as p_1 and p_2. The cutting tool rotates for a rotation angle of ϕ when it is fed from positions of p_1 to p_2.

Figure 10 The two positions of the cutting tool during the machining of a plane at a constant feed (see online version for colours)

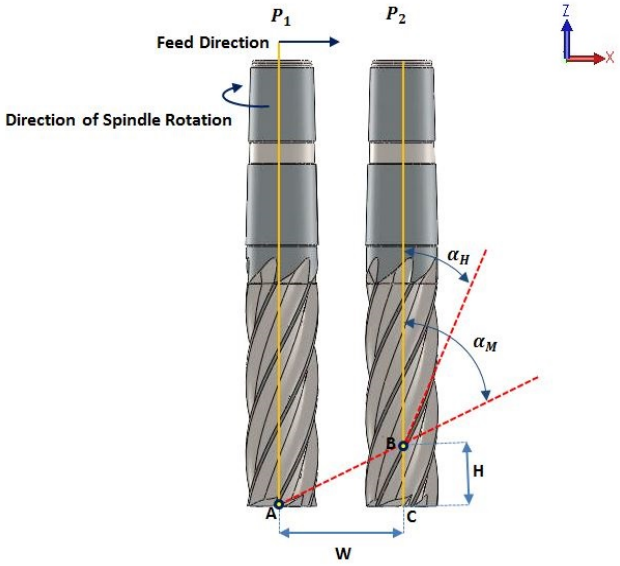

The distance between the two positions of the cutting tool as p_1 and p_2 can be presented as equation (20) (Dépincé and Hascoët, 2006a).

$$H = \frac{f\phi}{2\pi V_R} \tag{20}$$

where f is feed rate (mm/min), ϕ is rotation angle of the cutting tool and V_R is the tool rotation velocity (tr/min).

The height of the contact point B presented in Figure 10 can be shown as equation (21) (Dépincé and Hascoët, 2006a).

$$W = \frac{R\phi}{\tan\alpha_H} \tag{21}$$

where R and α_H are the tool radius and the helix angle, respectively.

The helix angle of the cutting tool can also be explained in equation (22) (Dépincé and Hascoët, 2006a).

$$\alpha_M = \tan^{-1}\frac{f\tan\alpha_H}{2\pi R V_R} \tag{22}$$

The trace of contact points is presented in Figure 11.

In the trace of contact points presented in Figure 11, two contact points of P_1 and P_2 are considered where the positions of them can be obtained by $\delta(Z_1,\phi_1)$ and $\delta(Z_2,\phi_2)$, respectively. The position z of the contact points can be presented as equation (23) (Dépincé and Hascoët, 2006a).

$$Z = \frac{R\phi}{\tan\alpha_H} \tag{23}$$

where R, ϕ and α_H are the cutting tool radius, rotation angle of the cutting tool and the helix angle of the cutting tool,

respectively. So, the trace of the contact point corresponding to the deformed profile is function of rotation angle of the cutting tool.

Figure 11 Trace of the contact points (see online version for colours)

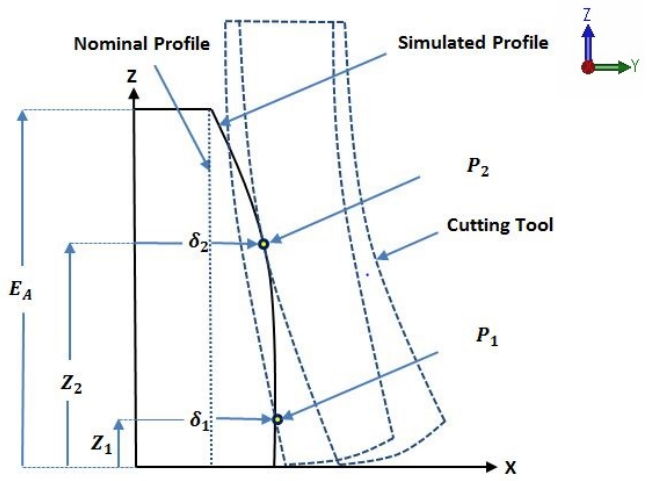

Three steps of the machined surface generation with the tool deflection error by using the contact point method are presented in Figure 12.

Figure 12 Three steps of machined surface generation with the tool deflection error by the contact point method (see online version for colours)

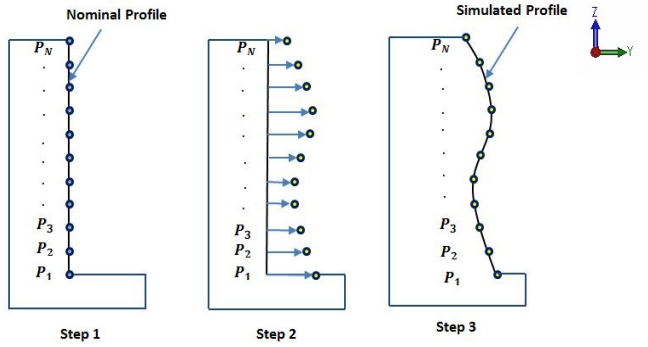

After considering the points on the nominal profile, new positions are calculated with respect to each tool's angular position. Then, the final milled profile can be obtained by a linear interpolation between the obtained contact points. The same procedure is repeated when the cutter is fed to a new position until the cutting tool leaves the workpiece. As a result, the simulated error surface due to tool deflection error can be presented by passing a surface from obtained contact points for each discrete position of the cutting tool along machining paths.

5 Virtual machining software to enforce the tool deflection error

The virtual machining software which can read and enforce tool deflection error to the nominal G-codes is developed in Visual Basic programming language. Nominal machining path, geometrics and materials properties of cutting tool as well as workpiece are input to the software. As a result, modified NC codes with tool deflection error are generated by the software using the calculated cutting forces at each position of cutting tool along machining paths. Then, modified version of the NC codes is used by a CAM software such as Vericut to create actual parts in virtual environment.

In order to analyse the tool deflection error by the FEM method, the software is linked to the FEM analysis software as Abaqus software. So, calculated cutting forces at each position of cutting tool along machining paths for workpiece and cutting tool are entered to the Abaqus software to be used in nodes displacement measuring. As a result, amount of the nodes displacement due to applied forces to the each node of meshed CAD models for cutting tool as well as workpiece are calculated as the tool deflection error.

Also, a developed algorithm is used to create the machined surfaces with tool deflection error generated by the method of contact points between cutting tool and workpiece.

The main dialog box of the software is shown in Figure 13 where the main and modified G-Codes are presented to the user.

Figure 13 Main dialog box of the software

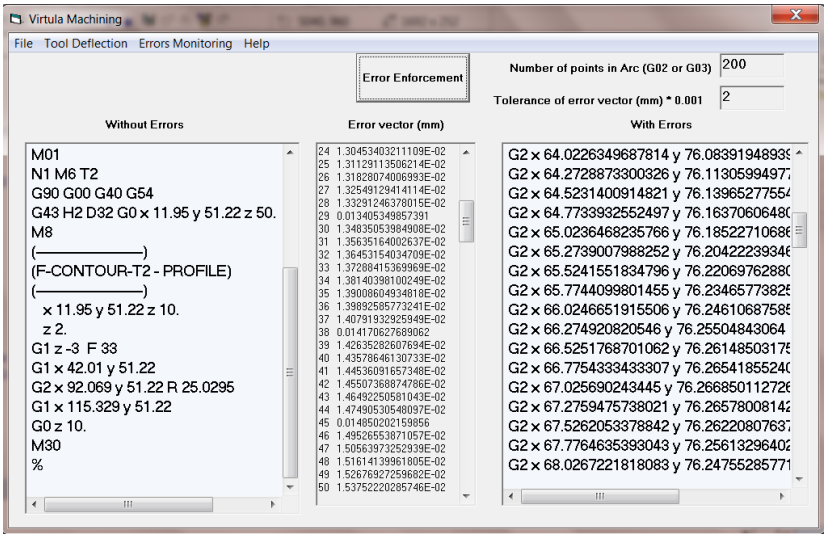

Figure 14 Dialog box of cutting force calculator for the cutting tool by using equation (4)

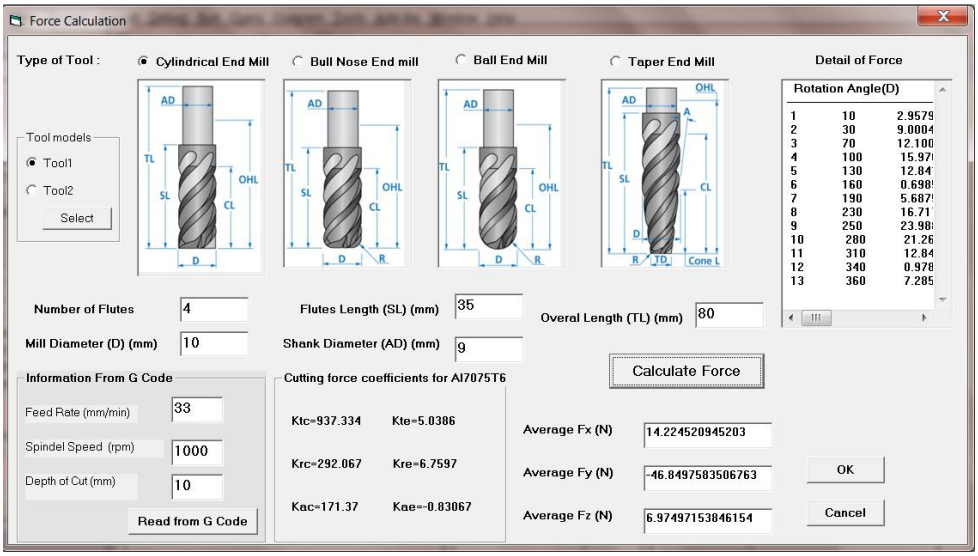

To calculate the tool deflection error, the cutting forces of the milling operation for each position of cutting tool along machining paths should be calculated. So, a dialog box is designed in the software to calculate cutting forces according to machining parameters as well as cutting tool details. The software considers four models of cutting tools due to different cutting edge angles in order to calculate the cutting forces. Figure 14 shows the cutting force calculator dialog box for the cutting tool by using the equation (4).

Cutting forces as *Fx*, *Fy* in equation (17) acting on the each axial segment engaged to the workpiece are also calculated by the software for each feed step as well as angular step of the cutting tool along machining paths. Then, calcualted cutting forces are used by the FEM analysis software in order to obtain deflections of the workpice as well as cutting tool. The algorithm of the software is presented in Appendix B.

6 Validation and comparison

In order to compare the reliability and accuracy of different methods of tool deflection errors modelling, the methods are experimentally tested by the virtual machining software. So, a free form profile is considered for machining and comparing in real and virtual environments. The test workpiece is machined by EMCO VMC600 CNC machine tool and measured by Zeiss CMM machine in order to find the difference of nominal and machined profiles. Measured data of CMM machine for the real part are compared with profiles of virtual parts obtained by using different methods of tool deflection errors modelling.

The cutting tool used in the experiment is HSS with materials of 16% tungsten, 5% chromium, 3% vanadium, 6% molybdenum and 8% cobalt. Type of the cutting tool is flat end mill with 10 mm diameter, helix angel 30°, flute number 4, overall length 89 mm and flute length 50 mm.

The workpiece material is AL7075T6. Profile of the test workpiece is shown in Figure 15. The spline profile has 0.33 mm radial and 10 mm axial depth of cut.

Figure 15 Profile of the test workpiece (see online version for colours)

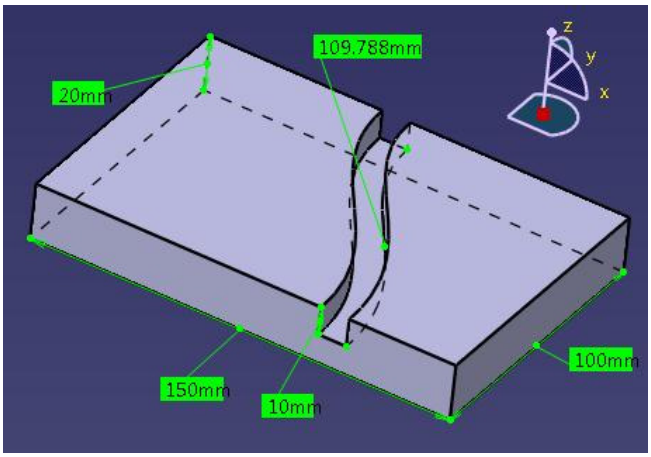

Figure 16 Measured cutting forces in slot milling tests, spindle rotating speed 1000 rpm

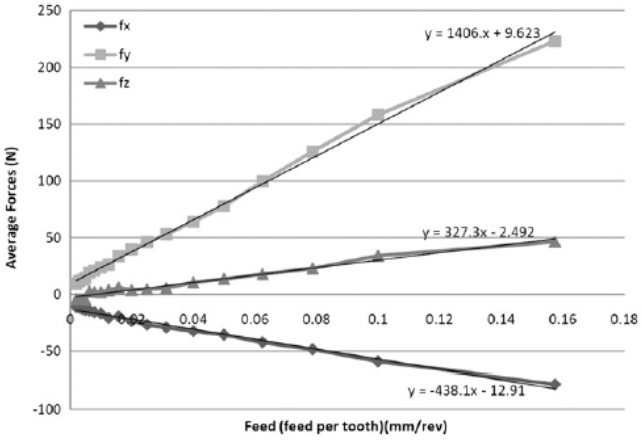

In this study, cutting force model of Engin and Altintas (2001) is used. The average of cutting force for 20 slot milling tests with 1.5 mm axial depth of cut is measured by Kistler dynamometer in order to estimate the cutting coefficients. By increasing the feed rate, the average of cutting forces increases linearly which shows a coherent relation between them. For fitting the experimental cutting forces with respect to feed rate, linear curve fitting is used and the diagram is obtained as Figure 16.

The cutting force coefficients are as equation (24).

$$\begin{aligned} K_{tc} &= 937.334, K_{te} = 5.0386 \\ K_{rc} &= 292.067, K_{re} = 6.7597 \\ K_{ac} &= 171.37, K_{ae} = -0.83067 \end{aligned} \tag{24}$$

In order to create virtual part with the tool deflection error, measured data and NC codes are supplied into the software to generate the error enforced G-Codes. Then, it is used on the same three-axis machine tool in Vericut software. After machining in Vericut, machined parts were inspected for contour errors at some designated key points by a CAD surface comparator software in order to find the errors of parts in virtual environment.

In order to analyse effects of the cutting forces to the workpiece, mesh generation is carried out to the CAD model of the workpiece by using Abaqus software. Then, predicted cutting forces at the each position of cutting tool along machining paths are applied to each node of the considered surface of the workpiece. As a result, effects of the cutting forces on the test workpiece by using the FEM analysis are shown in Figure 17.

Figure 17 Prediction of cutting forces effects on the test workpiece by using the FEM analysis

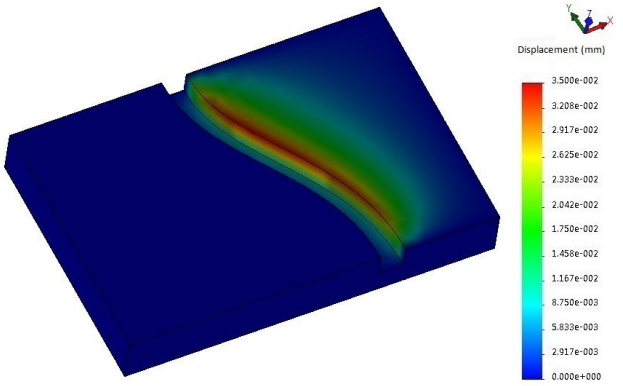

To calculate effects of the cutting forces on the cutting tool as the tool deflection error, CAD model of the cutting tool is considered. Mesh generation is carried out to the CAD model of cutting tool by using the Abaqus software to create 85,357 nodes and 56,628 elements. Material properties of the cutting tool in the FEM analysis are defined as Mass density, Yield strength and Poisson ratio with $7830\,\frac{ka}{m^3}$, $621231986\,\frac{N}{m^2}$ and $0.26\frac{N}{A}$, respectively. Calculated cutting forces are applied to the each node of the meshed model in order to measure nodes displacement. Prediction of cutting forces effects to the cutting tool as tool deflection error by using the FEM analysis is shown in Figure 18.

Figure 18 Prediction of cutting forces effects to the cutting tool as tool deflection error by using the FEM analysis

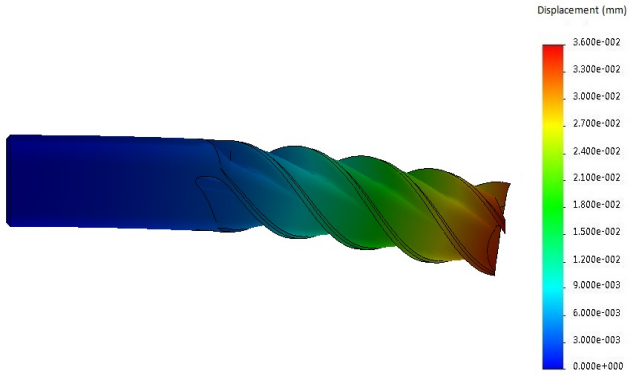

The measured tool deflection errors along the curve length for real and virtual parts are shown in Figure 19, where real part is machined part with tool deflection error in the real environment, FEM is virtual part with tool deflection error by considering effects of cutting forces to the cutting tool using the FEM analysis and CBM is virtual part with tool deflection error simulated by using the method of cantilever beam model of the cutting tool.

Figure 19 The measured tool deflection errors along the curve length for real and virtual parts

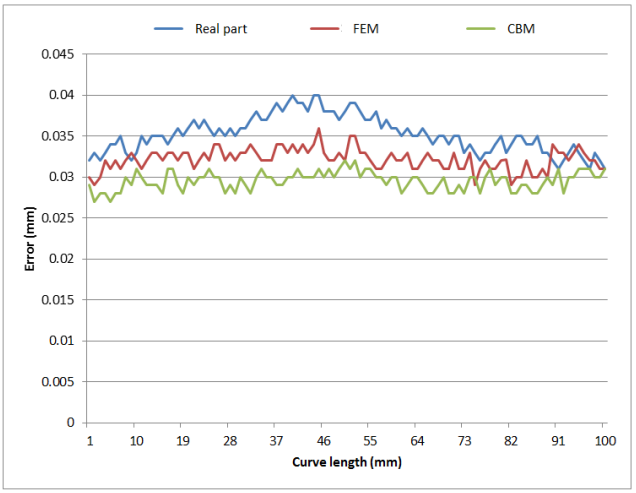

Distances between surfaces of nominal and real machined part with tool deflection error are shown in Figure 20.

By using the algorithm of the evolution of the contact points between cutting tool and workpiece, the surface of tool deflection error is created. As a result, distances between surfaces of nominal and virtual part with tool deflection error obtained by using evolution of the contact points between cutting tool and workpiece are shown in Figure 21.

Figure 20 Distances between surfaces of nominal and real machined part with tool deflection error

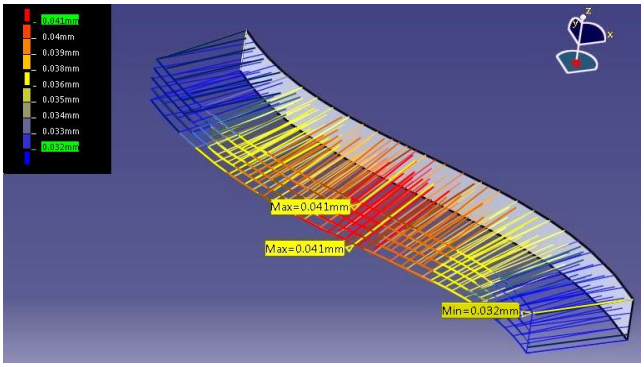

Figure 21 Distances between surfaces of nominal and virtual part with tool deflection error obtained by using evolution of the contact points between cutting tool and workpiece

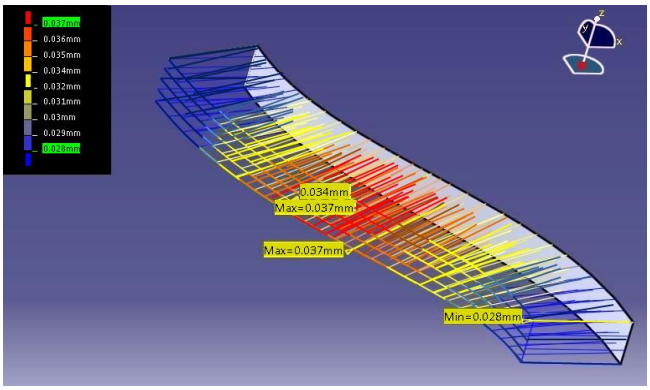

Distances between surfaces of real machined part and virtual part with tool deflection error obtained by using evolution of the contact points between cutting tool and workpiece are shown in Figure 22, where real part is machined part with tool deflection error in the real environment and virtual part is part with tool deflection error obtained by using evolution of the contact points between cutting tool and workpiece in virtual environment.

Figure 22 Distances between surfaces of real machined part and virtual part with tool deflection error obtained by using evolution of the contact points between cutting tool and workpiece

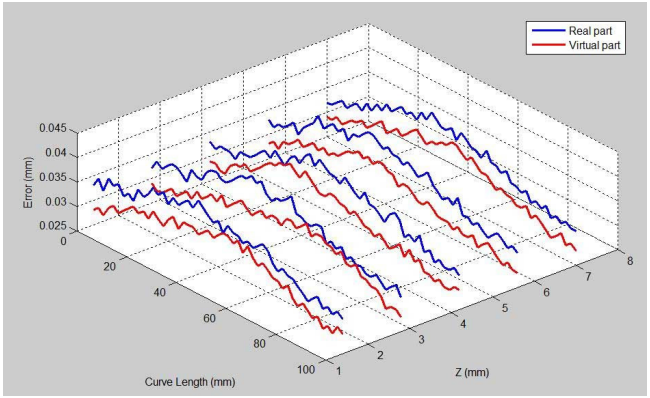

7 Conclusion

The research work presents an application for the virtual machining systems in order to analyse accuracy of tool deflection error modelling. A virtual machining system which can enforce tool deflection error of three-axis CNC milling machines is used to create real parts in the virtual environments. Different models of tool deflection are considered in order to show their accuracy and reliability in the error modelling. The results are compared to present the capabilities and difficulties of the methods in the tool deflection error modelling. As a result, 91.2%, 86.5% and 84.2% compatibility are obtained in comparison between real machined part and virtual parts obtained by the FEM method, cantilever beam model of the cutting tool and method of evolution of the contact points between cutting tool and workpiece, respectively.

The results show that the FEM can produce more accurate results by considering CAD models as well as materials properties of cutting tool and workpiece. So, cutting tool and workpiece with complex free form surfaces can be accurately analysed as a result of using the CAD models. But, the FEM needs modelling process for the cutting tool analysis in order to create the CAD model which makes the methods more complicated in comparison to the method of cantilever beam model of the cutting tool.

The cantilever beam model of the cutting tool is a quick method with less computational work to predict the tool deflection error. Also, deformation and deflection of tool clamping parts such as collet and arbour are considered in the tool deflection error of equation (5). But, different surfaces of cutting tool and effects of helical flutes of cutting tool to the machined surface are neglected in the method.

On the other hand, effects of helical flutes of the cutting tool to the machined surface are considered in tracing process of contact points in the method of evolution of the contact points between cutting tool and workpiece. But, implementation of the method in error modelling of complex surfaces has some difficulties due to obtaining a great number of the contact points.

Overall, it can be concluded that the FEM analysis is a powerful and efficient algorithm in order to provide an accurate analysis to the effects of cutting forces both on the cutting tool and workpiece. Complex geometries as well as material properties of cutting tool and workpiece can also be considered in the FEM analysis. Moreover, stress and strain of produced parts can be analysed by the FEM in order to determine the residual stress of machined parts.

Accuracy of error modelling can be studied with more complex cutting tools in milling operations of the five-axis CNC machine tools by analysing the effects of the tool deflection error on the workpiece. This is the concept of future research of the authors.

References

Altintas, Y., Brecher, C., Weck, M. and Witt, S. (2005) 'Virtual machine tool', *CIRP Annals-Manufacturing Technology*, Vol. 54, No. 2, pp.115–138.

Altintas, Y. and Merdol, S.D. (2007) 'Virtual high performance milling', *CIRP Annals-Manufacturing Technology*, Vol. 56, No. 1, pp.81–84.

Arizmendi, M., Fernández, J., Gil, A. and Veiga, F. (2009) 'Effect of tool setting error on the topography of surfaces machined by peripheral milling', *International Journal of Machine Tools and Manufacture*, Vol. 49, No. 1, pp.36–52.

Arsuaga, M., López de Lacalle, L.N., Lobato, R., Urbikain, G. and Campa, F. (2012) 'Force and deformation model for error correction in boring operations', *Advanced Materials Research*, Vol. 498, pp.121–126.

Budak, E. and Tekeli, A. (2005) 'Maximizing chatter free material removal rate in milling through optimal selection of axial and radial depth of cut pairs', *CIRP Annals-Manufacturing Technology*, Vol. 54, No. 1, pp.353–356.

Cao, Y. and Altintas, Y. (2007) 'Modeling of spindle-bearing and machine tool systems for virtual simulation of milling operations', *International Journal of Machine Tools and Manufacture*, Vol. 47, No. 9, pp.1342–1350.

Chen, C. and Zhao, G. (2016) 'Interpretation-oriented information interface for manufacturing enterprises', *International Journal of Computer Applications in Technology*, Vol. 53, No. 2, pp.189–195.

de Lacalle, L.L., Lamikiz, A., Sanchez, J.A. and Salgado, M.A. (2007) 'Toolpath selection based on the minimum deflection cutting forces in the programming of complex surfaces milling', *International Journal of Machine Tools and Manufacture*, Vol. 47, No. 2, pp.388–400.

Dépincé, P. and Hascoët, J.Y. (2006a) 'Active integration of tool deflection effects in end milling. Part 1. Prediction of milled surfaces', *International Journal of Machine Tools and Manufacture*, Vol. 46, No. 9, pp.937–944.

Dépincé, P. and Hascoët, J.Y. (2006b) 'Active integration of tool deflection effects in end milling. Part 2. Compensation of tool deflection', *International Journal of Machine Tools and Manufacture*, Vol. 46, No. 9, pp.945–956.

Engin, S. and Altintas, Y. (2001) 'Mechanics and dynamics of general milling cutters: Part I: helical end mills', *International Journal of Machine Tools and Manufacture*, Vol. 41, No. 15, pp.2195–2212.

Eskandari, S., Arezoo, B. and Abdullah, A. (2013) 'Positional, geometrical, and thermal errors compensation by tool path modification using three methods of regression, neural networks, and fuzzy logic', *The International Journal of Advanced Manufacturing Technology*, Vol. 65, Nos. 9–12, pp.1635–1649.

Fortunato, A. and Ascari, A. (2013) 'The virtual design of machining centers for HSM: towards new integrated tools', *Mechatronics*, Vol. 23, No. 3, pp.264–278.

Fu, H.J., DeVor, R.E. and Kapoor, S.G. (1984) 'A mechanistic model for the prediction of the force system in face milling operations', *Journal of Engineering for Industry*, Vol. 106, No. 1, pp.81–88.

Gogouvitis, X.V. and Vosniakos, G.C. (2015) 'Construction of a virtual reality environment for robotic manufacturing cells', *International Journal of Computer Applications in Technology*, Vol. 51, No. 3, pp.173–184.

Habibi, M., Arezoo, B. and Nojedeh, M.V. (2011) 'Tool deflection and geometrical error compensation by tool path modification', *International Journal of Machine Tools and Manufacture*, Vol. 51, No. 6, pp.439–449.

Ikua, B.W., Tanaka, H., Obata, F. and Sakamoto, S. (2001) 'Prediction of cutting forces and machining error in ball end milling of curved surfaces-I theoretical analysis', *Precision Engineering*, Vol. 25, No. 4, pp.266–273.

Liu, L.Y. and Wang, H.F. (2016) 'Integrated design and analysis system for feed drive system of CNC machine tools', *International Journal of Computer Applications in Technology*, Vol. 53, No. 2, pp.172–182.

Merdol, S.D. and Altintas, Y. (2008) 'Virtual cutting and optimization of three-axis milling processes', *International Journal of Machine Tools and Manufacture*, Vol. 48, No. 10, pp.1063–1071.

Nojedeh, M.V., Habibi, M. and Arezoo, B. (2011) 'Tool path accuracy enhancement through geometrical error compensation', *International Journal of Machine Tools and Manufacture*, Vol. 51, No. 6, pp.471–482.

Ong, T.S. and Hinds, B.K. (2003) 'The application of tool deflection knowledge in process planning to meet geometric tolerances', *International Journal of Machine Tools and Manufacture*, Vol. 43, No. 7, pp.731–737.

Rao, V.S. and Rao, P.V.M. (2006) 'Effect of workpiece curvature on cutting forces and surface error in peripheral milling', *Proceedings of the Institution of Mechanical Engineers, Part B: Journal of Engineering Manufacture*, Vol. 220, No. 9, pp.1399–1407.

Ratchev, S., Govender, E., Nikov, S., Phuah, K. and Tsiklos, G. (2003) 'Force and deflection modelling in milling of low-rigidity complex parts', *Journal of Materials Processing Technology*, Vol. 143, pp.796–801.

Ryu, S.H., Lee, H.S. and Chu, C.N. (2003) 'The form error prediction in side wall machining considering tool deflection', *International Journal of Machine Tools and Manufacture*, Vol. 43, No. 14, pp.1405–1411.

Saffar, R.J., Razfar, M.R., Zarei, O. and Ghassemieh, E. (2008) 'Simulation of three-dimension cutting force and tool deflection in the end milling operation based on finite element method', *Simulation Modelling Practice and Theory*, Vol. 16, No. 10, pp.1677–1688.

Soori, M., Arezoo, B. and Habibi, M. (2013) 'Dimensional and geometrical errors of three-axis CNC milling machines in a virtual machining system', *Computer-Aided Design*, Vol. 45, No. 11, pp.1306–1313.

Soori, M., Arezoo, B. and Habibi, M. (2016) 'Tool deflection error of three-axis computer numerical control milling machines, monitoring and minimizing by a virtual machining system', *Journal of Manufacturing Science and Engineering*, Vol. 138, No. 8, pp.081005.

Soori, M., Arezoo, B. and Habibi, M. (2014) 'Virtual machining considering dimensional, geometrical and tool deflection errors in three-axis CNC milling machines', *Journal of Manufacturing Systems*, Vol. 33, No. 4, pp.498–507.

Tsai, J.S. and Liao, C.L. (1999) 'Finite-element modeling of static surface errors in the peripheral milling of thin-walled workpieces', *Journal of Materials Processing Technology*, Vol. 94, No. 2, pp.235–246.

Wang, L. and Chen, Z.C. (2014) 'A new CAD/CAM/CAE integration approach to predicting tool deflection of end mills', *The International Journal of Advanced Manufacturing Technology*, Vol. 72, Nos. 9–12, pp.1677–1686.

Yucesan, G. and Altıntaş, Y. (1996) 'Prediction of ball end milling forces', *Journal of Engineering for Industry*, Vol. 118, No. 1, pp.95–103.

Yun, W.S., Ko, J.H., Cho, D.W. and Ehmann, K.F. (2002) 'Development of a virtual machining system, part 2: prediction and analysis of a machined surface error', *International Journal of Machine Tools and Manufacture*, Vol. 42, No. 15, pp.1607–1615.

Zeroudi, N. and Fontaine, M. (2015) 'Prediction of tool deflection and tool path compensation in ball-end milling', *Journal of Intelligent Manufacturing*, Vol. 26, No. 3, pp.425–445.

Appendix A

$$\begin{cases} dF_x\left(\phi_j\right) = -dF_t \cos\phi_j - dF_r \sin\phi_j \\ dF_y\left(\phi_j\right) = +dF_t \sin\phi_j - dF_r \cos\phi_j \\ dF_z\left(\phi_j\right) = +dF_a \end{cases} \quad \text{(A.1)}$$

Appendix B

1: Input

Read the G-Code file

Split the G-Codes to recognise the elements (G01, G02, G03, X, Y, Z, R, …)

2: Calculation of cutting forces

Read machining parameters (Feed rate, Depth of cut, Spindle Speed) from G-Codes file

Select kind of cutting tool (Flat end, Ball nose end, Ball end, Taper end) by user

Import cutting tool details (Lengths, Number of flutes, Diameters) by user

Select material of workpiece for cutting force coefficient (K_{tc}, K_{rc}, K_{ac}, K_{te}, K_{re}, K_{ae})

Calculate cutting forces as *Fx*, *Fy*, *Fz* presented in equation (4) for different rotation angels of tool cutting edge between entering and existing angles for each position of cutting tool along machining paths

3: Error Enforcement

Calculate amount of tool deflection errors by calculated cutting force for each position of cutting tool along machining paths

Add amount of tool deflection errors to G-Codes

4: Write file

Join the new G-Codes

5: Output

Save as new G-Codes

6: FEM analysis

Import material properties of the workpiece by the user

Use meshed CAD model of the workpiece generated by the Abaqus software

Determine stiffness matrix of the workpiece

Calculate cutting forces as *Fx*, *Fy* presented in equation (17) acting on the each axial segment engaged to the workpiece for each feed step as well as angular step of the cutting tool along machining paths

Use the calculated cutting forces as *Fx*, *Fy* presented in equation (17) for FEM analysis of the workpiece

Use calculated cutting forces as *Fx*, *Fy*, *Fz* presented in equation (4) for different rotation angels of tool cutting edge between entering and existing angles for each position of cutting tool along machining paths for FEM analysis of the cutting tool

Transfer the calculated cutting forces at each position of cutting tool along machining paths to the Abaqus software

Receive the reports of the FEM analysis for the nodes displacement

7: Approach based on evolution of the contact points between cutting tool and workpiece

Determine contact points between the workpiece and the cutting tool flute for each Z, ϕ of machining paths

Calculate amount of the $\delta\left(Z,\phi\right)$ for each contact point between the workpiece and the cutting tool flute

Pass the simulated surface by applying a linear interpolation between obtained contact points between the workpiece and the cutting tool flute.

8: Comparison

Compare obtained results by charts and diagrams.